

Mars Atmosphere and Volatile Evolution (MAVEN) Mission

Anomaly Review Board (ARB) Report

FINAL REPORT CONTRIBUTORS

Hoppy Price, NASA Jet Propulsion Laboratory, California Institute of Technology, Chair
Carmel Conaty, NASA HQ OCE
Jesse Bullock, NASA GSFC
Joel Krajewski, UC Berkeley
Tim McElrath, NASA Jet Propulsion Laboratory, California Institute of Technology
Liam Pisano, NASA GSFC
Devin Poland, NASA GSFC
Eric Siskind, NASA GSFC
Chris Waters, Lockheed Martin
Charles Whetsel, NASA Jet Propulsion Laboratory, California Institute of Technology

JULY 17, 2026

This research was carried out at the Jet Propulsion Laboratory, California Institute of Technology, under a contract with the National Aeronautics and Space Administration (80NM0018D0004).

© 2026. All rights reserved.

TABLE OF CONTENTS

Sections

1 Executive Summary 1-1
2 Mission Overview 2-1
3 Spacecraft Design 3-1
4 Observed Events 4-1
5 Anomaly Fishbone Analysis 5-1
5.1 Elimination of Fishbones 5-1
5.2 Inertial Measurement Unit Functional Description 5-2
5.3 IMU Failure Scenario 5-4
5.4 MAVEN's History of IMU Anomalies 5-4
5.5 STEREO-B Anomaly 5-6
5.6 STEREO-B Anomaly Relationship to MAVEN LOS 5-7
5.7 Simulation of a Faulty IMU Output 5-7
6 Root Cause Assessment 6-1
6.1 Probability of an SEU 6-1
6.2 External Impact Analysis 6-2
6.3 Assessment of the Most Likely Scenario 6-3
7 Findings and Recommendations 7-1
7.1 Assessment of MAVEN's Orbit and Stability 7-1
7.2 Assessment of Orbital Debris and Potential Hazards 7-1
7.3 Addressing IMU Vulnerabilities and End of Life 7-1
7.4 Gyroless Modes of Operation 7-2
7.5 Fault Protection Recommendations 7-2
7.6 Space Situational Awareness at Mars 7-2

Figures

3-1 The MAVEN spacecraft showing the body-fixed antennas and solar arrays 3-1
3-2 Early stage in assembly of the MAVEN spacecraft, showing the core structure being lowered onto the main propellant tank that sits within the center core 3-2
3-3 The central body of the MAVEN spacecraft showing the TCM thrusters 3-3
4-1 Doppler data showing changes in velocity (ΔV) events 4-2
5-1 Potential spacecraft faults are shown in a fishbone diagram 5-1
5-2 The Honeywell MIMU 5-2
5-3 Simplified diagram of a ring laser gyroscope 5-3
5-4 MAVEN's IMU-2 laser intensity monitor 5-4

Appendices

A Convening Memo A-1
B Integrated Timeline of Anomaly Events B-1
C Acknowledgment C-1
D Acronyms D-1
E References E-1

1 EXECUTIVE SUMMARY

On December 6, 2025, the Mars Atmosphere and Volatile Evolution (MAVEN) spacecraft was in normal operations with no indications of any problems or issues. During a routine occultation when the spacecraft passed behind the planet of Mars, out of communication with the Earth, it experienced an anomaly that resulted in the vehicle tumbling between about 2.7 and 2.3 revolutions per minute (RPM) and in a safe mode, transmitting on its low-gain antenna (LGA). When the spacecraft emerged from behind the planet, the LGA and solar arrays were significantly off-pointed from the Earth and the Sun, resulting in a weak signal, as received from the tracking station, and with the solar arrays unlikely to keep the spacecraft power positive for more than about 12 hours. The last signal received from MAVEN occurred about 4 hours and 20 minutes after the suspected time of the anomaly's initiation.

Beginning 21 hours after the anomaly, the project team made multiple attempts to recover the spacecraft by broadcasting commands to put it in a recoverable state, but no responses were received from the vehicle. Over many days, attempts were made to listen for any faint signals from MAVEN using the Deep Space Network (DSN) and the Green Bank Observatory, but no signals were detected.

The fundamental objective of this anomaly investigation was to understand the state of the spacecraft, identify potential causes of the anomaly, identify any potential hazards to the Mars orbital environment, and make recommendations on how to minimize the potential for future similar mishaps.

The Anomaly Review Board (ARB) was briefed by the MAVEN project and Lockheed Martin (LM) as part of their investigation into the failure. Given the sparsity of telemetry data available from MAVEN following the anomaly, the ARB could not conclusively identify a single specific root cause and could only identify a likely root cause.

The ARB believes that the anomaly was most likely initiated by either (1) a radiation-induced single-event upset (SEU) or (2) a software issue, causing an unrequested reboot of the flight computer. The reboot powered up the inertial measurement unit (IMU), which then failed to provide correct attitude rate data, causing the spacecraft to spin itself up in response to the faulty data. The spacecraft was not able to recover from this spin state. This scenario has similarities to the IMU failure experienced by the STEREO-B spacecraft in 2014, which resulted in it also tumbling in an unrecoverable state.

MAVEN was performing its sixth extended mission after operating at Mars for over 11 years, 8 years beyond its designed mission. Both of its IMUs were operating at end-of-life conditions, and the project was actively performing mitigation measures to protect the spacecraft's operation by implementing a gyroless mode that used a star tracker for attitude reference, bypassing the IMUs, and by making innovative changes to the fault protection algorithms. Even so, the spacecraft was vulnerable to the condition of not having a functioning

IMU following a spacecraft reboot, and this was understood by the project and the Mars Exploration Program.

The ARB believes that the spacecraft is likely in an intact condition in a stable orbit and presents no unusual debris hazards or risks to other vehicles in Mars orbit. This is inferred by the fact that MAVEN was still functioning for over 4 hours after the initiation of the anomaly.

The ARB has identified items that may have been contributing causes with recommendations to minimize the likelihood of a similar problem on future missions. These findings and recommendations are summarized in Chapter 7 of this report.

2 MISSION OVERVIEW

The MAVEN project was a competed mission in NASA's Mars Scout Program. The primary science objective was to study the Martian atmosphere, characterize its properties, measure the rate of loss of gas, and provide data to reconstruct the history of how the atmosphere evolved over the past 4 billion years.

MAVEN is a Principal Investigator–led mission from the University of Colorado Laboratory for Atmospheric and Space Physics. Goddard Space Flight Center (GSFC) is the lead NASA center responsible for the project's management. LM is the spacecraft provider and operator under contract from GSFC.

MAVEN was designed as a three-axis stabilized spacecraft with mostly body-fixed components except for an articulated instrument platform on a boom (see Figure 3-1). The spacecraft bus houses the spacecraft avionics, power system (including solar arrays), propulsion system, and telecommunication system.

MAVEN was launched November 18, 2013, on an Atlas V rocket from Kennedy Space Center. It used its propulsion system to enter Mars orbit on September 22, 2014. The spacecraft began its science operations on November 16, 2014, and it subsequently fulfilled its primary mission to operate for one Martian year. It was approved for a continuing series of extended missions and was in Extended Mission 6 at the time of the anomaly.

On December 6, 2025, the spacecraft was functioning normally when it had a routine orbital event passing behind Mars, as observed from Earth. During this occultation event, the vehicle was out of communication with the Earth. When it emerged from behind the planet, 31 minutes later, there was only a weak signal from the spacecraft with very limited sporadic segments of telemetry picked up by the DSN. The MAVEN team executed the loss of signal (LOS) contingency procedure, and when the initial recovery steps were not successful, a spacecraft emergency was declared. All following attempts to command the vehicle or receive a signal were unsuccessful.

NASA formed the ARB to investigate the incident. Most of the analyses and simulations described in Section 6 were performed by LM. Many of the ARB's assessments and conclusions about the technical nature of the anomaly benefited from the interactions with the project and LM.

3 SPACECRAFT DESIGN

The MAVEN spacecraft design blended heritage from previous LM spacecraft, including Juno, Grail, and Mars Reconnaissance Orbiter, with a mission-unique configuration driven by the science instrument accommodation requirements.

The spacecraft is three-axis stabilized, with an articulated payload platform (APP) deployed on a 1.2-m boom (Figure 3-1). This configuration allows pointing some instruments relative to the Sun or to the solar wind, while simultaneously pointing others relative to the planet or atmosphere. The former instruments are fixed on the spacecraft or on fixed booms, and the spacecraft is generally operated with its solar arrays pointed toward the Sun.

The solar arrays and high-gain antenna (HGA) are fixed to the spacecraft body. The spacecraft and the solar arrays would nominally point at the Sun and could be pointed toward the Earth during communication windows.

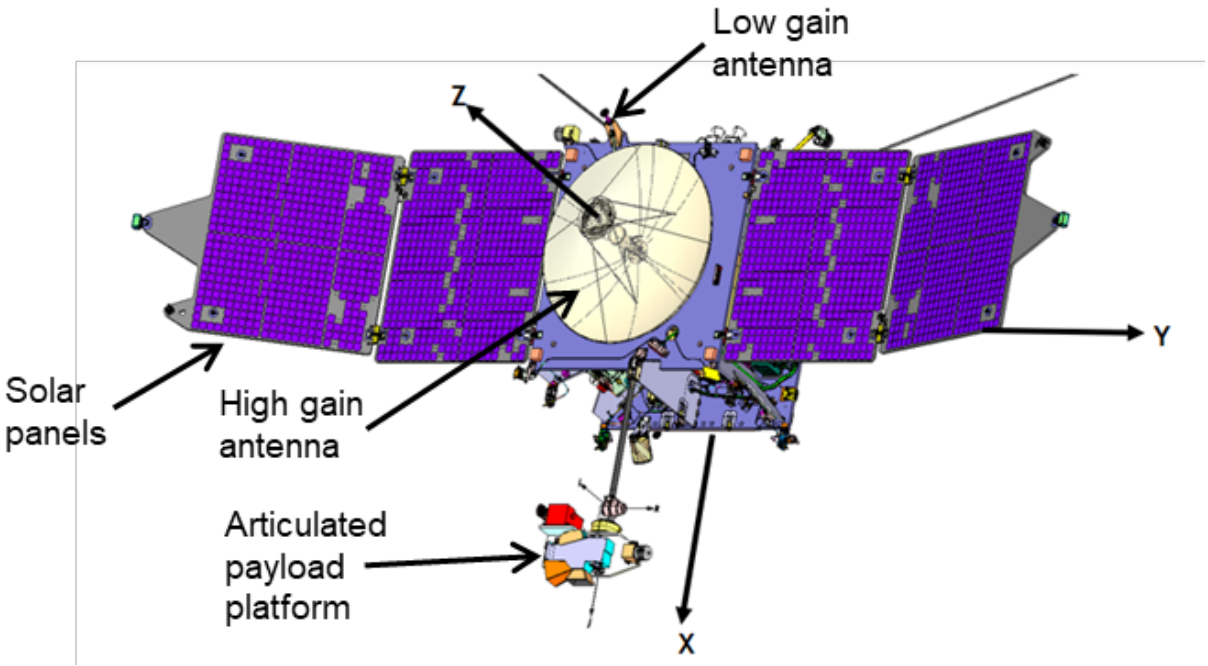


Figure 3-1. The MAVEN spacecraft showing the body-fixed antennas and solar arrays.

In addition to the HGA, two LGAs provide essentially full-sky coverage. The LGA next to the HGA has its boresight 22.5° off-pointed from the HGA. The LGAs were used to communicate with the spacecraft in safe mode, and to allow communications for tracking during science operations.

The spacecraft structure is aluminum honeycomb composite, with a cylindrical core that encloses the hydrazine fuel tank at the center of the body (Figure 3-2). The primary structure surrounding the core has four open bays that allowed easy access to the spacecraft components

during assembly and testing. Individual components were mounted at fixed locations on the primary structural panels.



Figure 3-2. Early stage in assembly of the MAVEN spacecraft, showing the core structure being lowered onto the main propellant tank that sits within the center core.

The solar arrays were designed with a split, gull-wing configuration to provide an offset between the spacecraft center of mass and the center of force for aerodynamic stability during passages through the upper atmosphere for science data collection.

The attitude control system (ACS) used a combination of reaction wheels and thrusters. The propulsion system was hydrazine monopropellant pressurized by helium. Mars orbit insertion (MOI) was carried out with six thrusters located on the rear of the spacecraft that were isolated from the rest of the propulsion system following orbit insertion. Four trajectory correction maneuver (TCM) thrusters were used to adjust both periapsis and apoapsis of the orbit, while eight ACS thrusters controlled the spacecraft attitude and removed accumulated momentum from the reaction wheels (Figure 3-3).

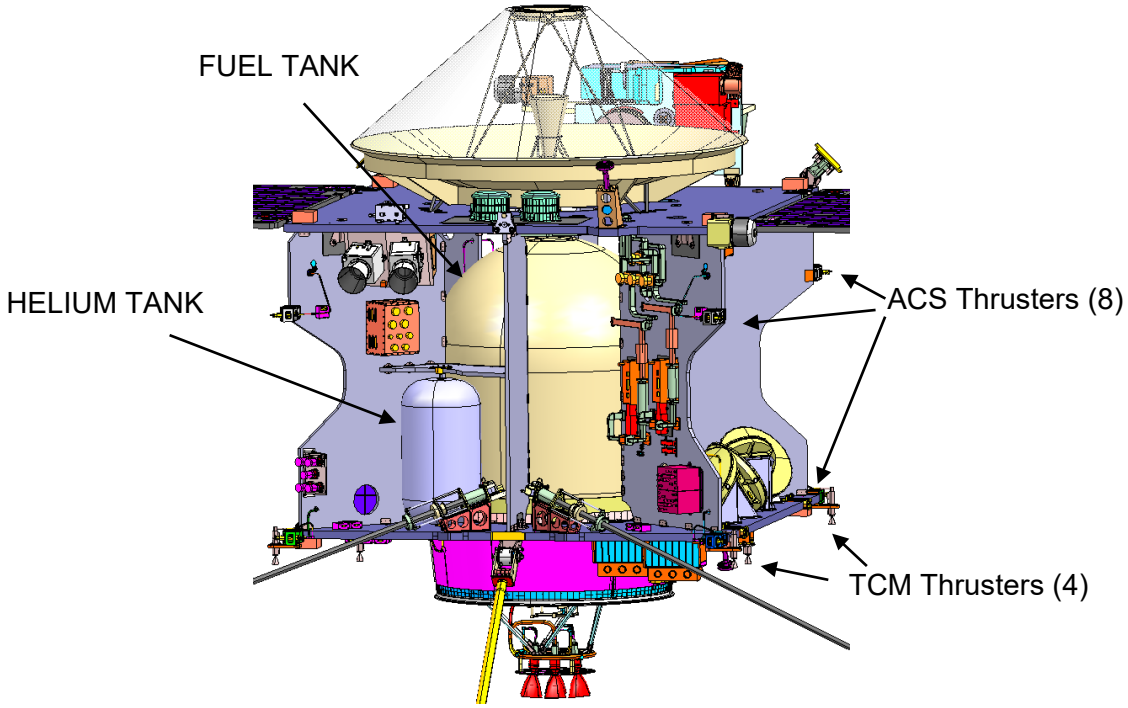


Figure 3-3. The central body of the MAVEN spacecraft showing the TCM thrusters.

4 OBSERVED EVENTS

The basic events are summarized here, but a detailed timeline is provided in Appendix B.

The MAVEN spacecraft emerged from behind Mars at 2:29 Coordinated Universal Time (UTC), Earth-received time (ERT). The one-way light time to Earth was 20 minutes and 9 seconds. The signal received from the spacecraft by the DSN was very weak with the signal changing in magnitude in a sinusoidal pattern. Because of the weak signal, no data were obtained in real time.

Fortuitously, the science team was performing a radio science experiment and was recording the received signal, in what is termed open-loop recording (OLR), as a raw signal that does not require a lock with the spacecraft's transponder. Several days after the anomaly, the OLR data were processed to recover some additional telemetry and Doppler shift data [1].

Telemetry received from the spacecraft included indications that the vehicle had experienced an unrequested reboot of the flight computer, that MAVEN was in safe mode, that attitude control was requesting another reboot, and that the spacecraft was tumbling at a rate of about 2.7 RPM [2].

Subsequent investigation revealed the following information:

1. The radio science data indicated that when MAVEN exited occultation after the anomaly, it had experienced an anomalous change in velocity. The magnitude of the ΔV is difficult to determine, but it was estimated to have been at least 0.2 m/s and could have been as high as 1.4 m/s or more.
2. The sinusoidal signal strength variation received at Earth indicated that the spacecraft was rotating with a rate of about 2.7 RPM. This also matched telemetry from the inertial measurement unit (IMU-2).
3. The spacecraft was stuck in an attitude control fault protection cycle of trying and failing to de-tumble the vehicle. The repeating cycle began with two attempts (4 minutes apart) to de-tumble using the small reaction control system (RCS) thrusters, followed by two attempts (4 minutes apart) to de-tumble using the larger TCM thrusters. The four failed de-tumble attempts were then followed by a requested computer reboot and then safe mode entry. Then the cycle of four de-tumble attempts (each 4 minutes apart) followed by a reboot would repeat.
4. In each de-tumble attempt cycle, the first TCM thruster attempt reduced the spin rate from 2.7 rpm to about 2.3 rpm. The second TCM thruster attempt restored the spin rate to 2.7 rpm. This was observed in the radio science data and seems to be consistent throughout the repeating cycles.

5. Changes in spacecraft velocity were observed in the Doppler shift of the radio signal that coincided with the expected times of the de-tumbling thruster firings (4 minutes apart) in the cycle described above.

The MAVEN project followed procedures for recovering the spacecraft after an LOS event. Actions taken following the anomaly are summarized below:

1. A command was sent to MAVEN at 23:09 UTC to power on the radio system and transmit to Earth.
2. Commands were sent to enter safe mode, swap sides on the redundant transmitters and receivers, and swap antennas.
3. A command was sent to force a spacecraft reboot.

No responses from MAVEN were ever received.

The radio science OLR data provided Doppler data, which if properly interpreted can indicate changes in the velocity of the spacecraft. Figure 4-1 shows the change in Earth line-of-sight frequency of the spacecraft antenna, compared to an unperturbed reference trajectory. Because of the Doppler effect on the radio signal, these changes can be interpreted as line-of-sight velocity differences. Each segment of Doppler data shows an oscillatory behavior that is understood to be due to the spacecraft rotation, punctuated by shifts in the mean (marked with a "ΔV" symbol) that are understood as discrete velocity changes. This signature, as well as the gaps, is consistent with the attitude control fault protection behavior described above.

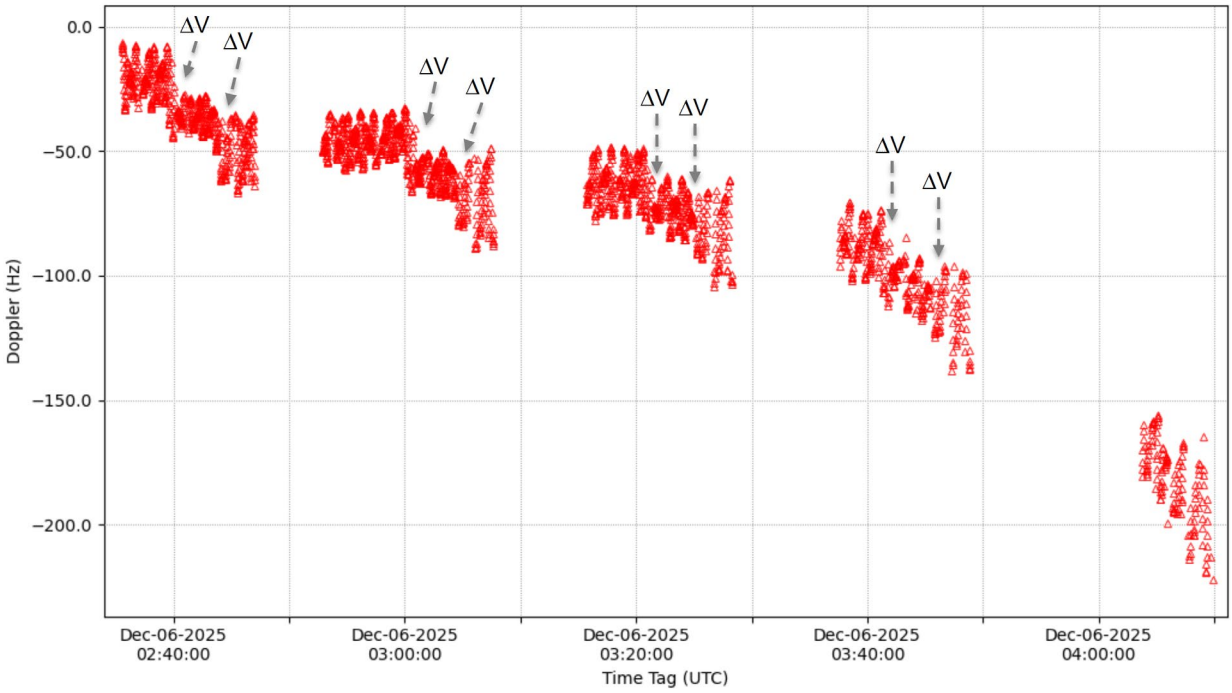


Figure 4-1. OLR Doppler data showing velocity change (ΔV) events.

The line-of-sight velocity change of each event is about 0.25 m/s. The total velocity change could be higher, but there is no way to estimate that with the data available. The spin rate between each pair of ΔV events is either ~2.7 rpm, or ~2.3 rpm, as discussed in the TCM thruster de-spin cycle described above. The smaller envelope that occurs between each closely spaced pair of ΔVs indicates that the spin rate there is slower.

The quality of the Doppler data starts out relatively strong and then degrades over the timespan shown in Figure 4-1. Consequently, it becomes more difficult to detect ΔVs and spin rates as time passes. In addition, these ΔVs, as well as others that are thought to have occurred during geocentric occultation, have perturbed the trajectory such that the line-of-sight velocity shows an increasing difference with respect to the unperturbed reference trajectory, which makes finding discrete ΔVs more difficult.

5 ANOMALY FISHBONE ANALYSIS

LM developed a fishbone diagram of potential spacecraft faults that could result in the anomaly (see Figure 5-1). This was done by looking for failures that could cause excessive spin rate.

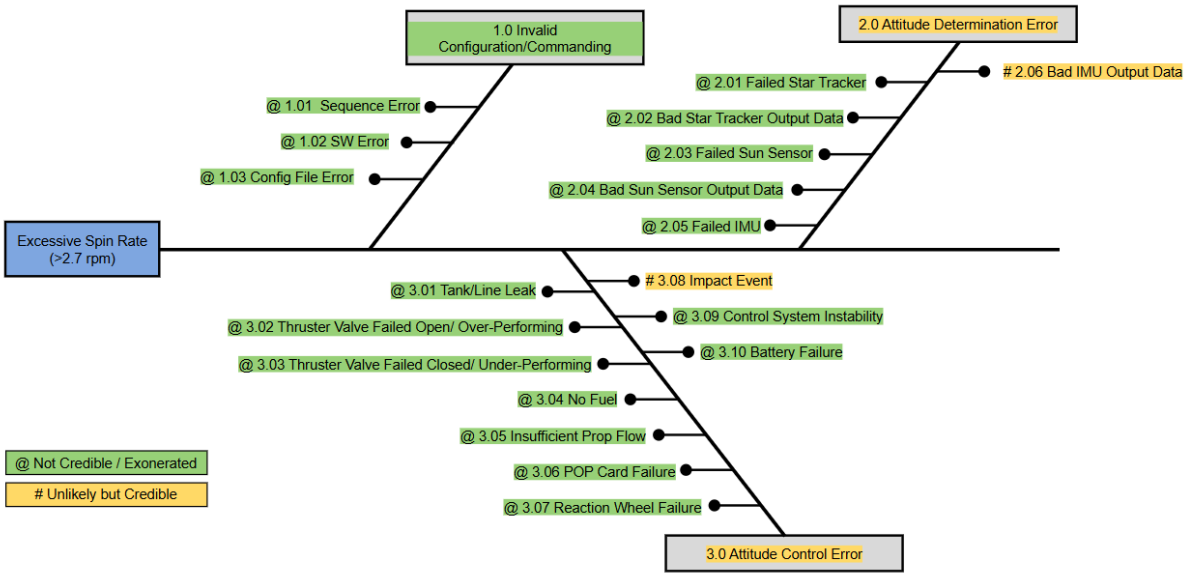


Figure 5-1. Potential spacecraft faults are shown in a fishbone diagram.

5.1 ELIMINATION OF FISHBONES

The MAVEN project and LM have systematically eliminated most of the items in the fishbone by analysis, simulations, and data from the telemetry and OLR analyses. These are summarized as follows:

- **Sequence error, software error, or configuration file error.** These were all examined and exonerated as causes.
- **Failed star tracker or bad output.** A star tracker failure would not result in the spacecraft spinning at the observed rate.
- **Failed sun sensor or bad output.** Sun sensor output was not used in the observed timeline, so they could not stimulate high rates.
- **Propulsion system leakage.** Leakage would require multiple failures of valve seals and is not supported by any evidence.
- **Propulsion system rupture or puncture.** Observables indicate discrete ΔV events, many of which correspond to rate damp periods that suggest close-to-nominal thruster performance for 1–2 hours post-occultation exit. This is in contradiction with any leakage event that would eliminate or degrade thruster performance by that time.
- **Thruster valve failure.** A failed open thruster would provide a continuous force on the vehicle up to fuel depletion that would have shown up in the Doppler signature, and that did not occur.

- **Propulsion valve driver failure.** Driver failure would require two faults, which is not a credible scenario with no in-flight history of issues.
- **No remaining propellant or insufficient flow.** A simulation of continuing de-spin attempt cycles estimated 7.4 kg of propellant usage, so MAVEN had plenty of available propellant at the initiation of the anomaly.
- **Reaction wheel failure.** A reaction wheel failure would not result in the spacecraft spinning at the observed rate.
- **Control system instability.** Responses to instability would be primarily oscillatory and do not fit the observed timeline derived from the radio signal.
- **Battery failure (e.g., runaway thermal event).** Telemetry before and after occultation does not indicate any anomalous battery conditions. Radio signals imply that the spacecraft was successfully powered by the battery for at least 4 hours after the anomaly.

The following discussion describes the functioning of the IMUs, as these were a known risk and could be a credible cause of the failure.

5.2 Inertial Measurement Unit Functional Description

MAVEN was equipped with two miniature inertial measurement units (MIMUs) from Honeywell Aerospace, which measure rotation rate using three ring-laser gyroscopes (RLGs), as well as acceleration in three axes (Figure 5-2). A high-level understanding of the RLG design is necessary to explain one of the leading potential causes of the MAVEN LOS.



Figure 5-2. The Honeywell MIMU.

An RLG is an optical device that measures angular velocity by exploiting the Sagnac effect, a phenomenon in which two light beams traveling in opposite directions around a rotating loop experience a relative phase shift. The different beams are combined to form an interference pattern that can be read out by a detector. A simplified diagram of an RLG is shown in Figure 5-3.

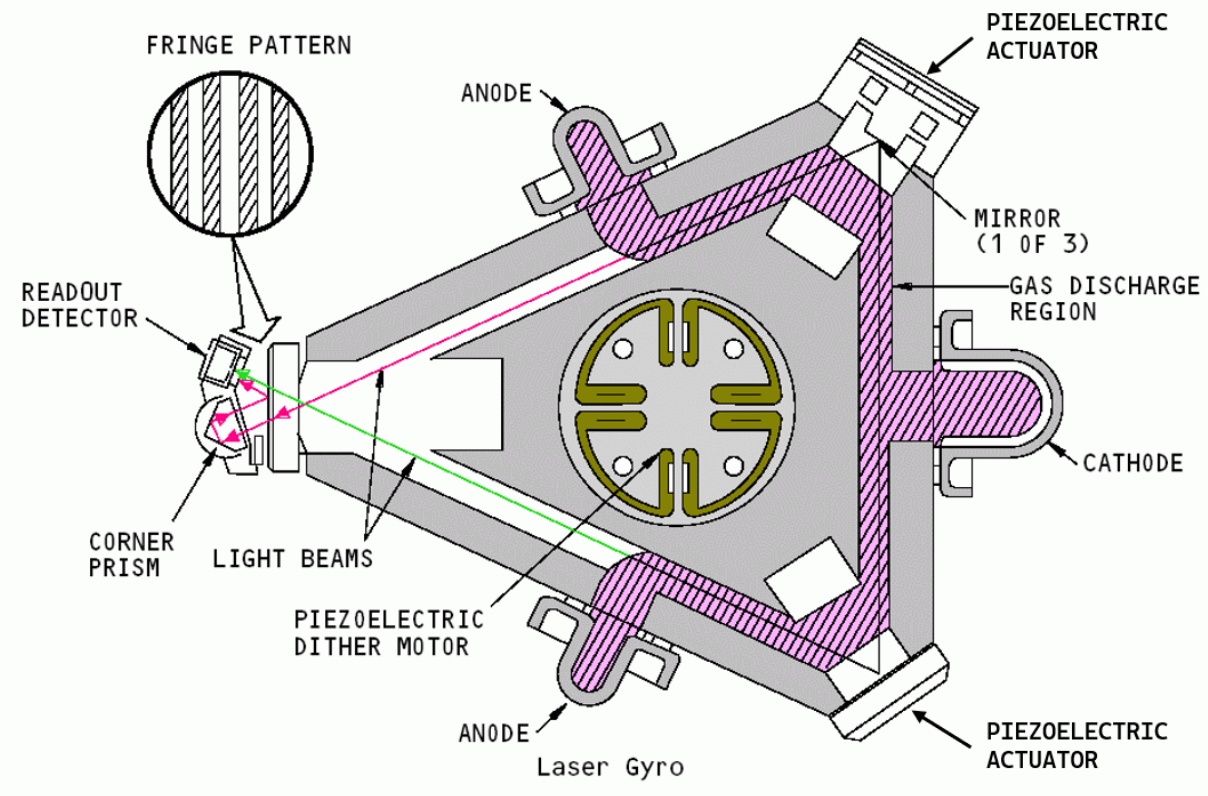


Figure 5-3. Simplified diagram of a ring laser gyroscope.

RLGs are complicated devices with moving parts, pressurized gases, and high-voltage electrical components. Of particular interest for the upcoming section on the potential IMU failure are these parts of the internal control loops and diagnostics of the MIMU:

1. Path length control (PLC) uses piezoelectric actuators to move the mirrors in the upper and lower right corners of the diagram, making micro adjustments to the length of the path each laser must travel in order to focus the beams to form a clear interference or fringe pattern.
2. The single-beam signal (SBS) is a measure of the individual laser beams before they are combined. This information is used in the RLG's internal control loop.
3. The laser intensity monitor (LIM) measures the optical intensity of the laser and is a good indicator of laser health.

5.3 IMU Failure Scenario

When considering an IMU failure and its role in the overall LOS scenario, an unrelated event must have initially triggered the spacecraft's entry into safe mode. Prior to the anomaly, the IMU was neither powered nor in use, as MAVEN was operating in its gyroless mode. This mode used a star tracker for attitude reference rather than the gyros, and is also known as the all-stellar mode. The gyroless software was not capable of running during a safe mode event, so a functioning IMU was required to control rates, and one was powered up for use. The IMU failure scenario described in this section likely transformed a potentially recoverable safe mode entry into a mission-ending event.

There is a known IMU failure scenario, observed on the STEREO-B spacecraft, that produces no real rate signal but outputs noise with a non-zero offset. Because the ACS cannot distinguish this from a real measurement, it continuously attempts to correct for the offset, spinning the spacecraft up indefinitely. This could explain the periodic radio signal observed when MAVEN came back into view, as well as the observed timing of safe mode re-entries and thruster firings described in Section 4, and was shown to match simulations well.

5.4 MAVEN's History of IMU Anomalies

MAVEN was equipped with two MIMUs from Honeywell Aerospace, which measure rotation rate using three RLGs. The primary unit, IMU-1, was removed from regular operation approximately eight years into the mission when it began experiencing frequent laser PLC resets in one axis, a pattern that Honeywell identified as indicating imminent failure.

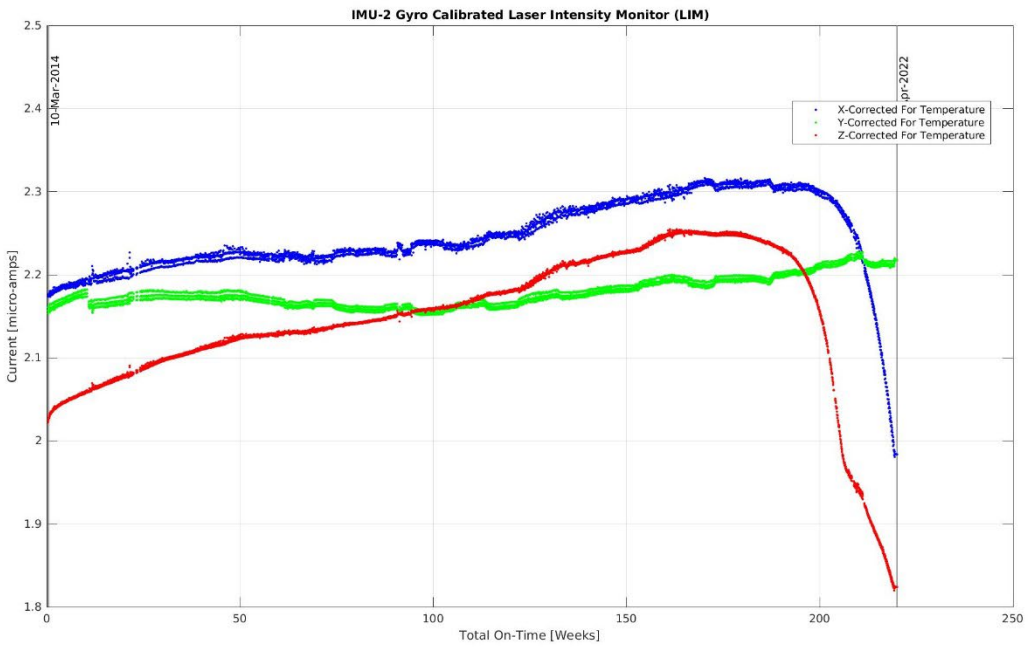


Figure 5-4. MAVEN's IMU-2 laser intensity monitor.

With IMU-1 removed from service, IMU-2 became a single-string failure point, prompting the project to begin planning for a software patch to add a gyroless control mode. In 2021, IMU-2 began showing signs of laser end-of-life degradation in two axes (see Figure 5-4). As a result, the gyroless control development that was already underway was accelerated and successfully uploaded in April 2022.

It is noteworthy that both MIMUs exhibited end-of-life characteristics after approximately 6 years of operation, a shorter lifetime than expected, and consistent between units. While no guaranteed operational life is published, based on industry expectations, a Honeywell MIMU is expected to have a serviceable lifetime of 10–15 years or more in operational use. The published operational temperature range is −30°C to 65°C, and MAVEN had been operating with a steady-state internal temperature around 40°C. Honeywell later explained that the sustained higher operating temperatures had likely accelerated degradation, even though the units were operated within the published temperature range. The original specifications did not state that sustained operation at the warmer end of the acceptable range would shorten unit life. Had the project known this, alternate MIMU placement could have extended their lifetimes and potentially the mission.

In July 2021, while the gyroless patch was still under development, the program reactivated IMU-1 in an effort to preserve the remaining life on IMU-2. After about 30 days, hundreds of PLC resets occurred within a few hours. The team switched back to IMU-2.

At Honeywell's suggestion, in February 2022, the team returned to IMU-1 with a strategy of power cycling the unit twice per week to prevent the PLC resets. After about 2 weeks, IMU-1 failed to power back up successfully and the spacecraft spent about 70 minutes in a safe mode and power cycle loop. When IMU-2 was autonomously powered on, it produced brief out-of-spec rate noise that triggered a flight software "sanity check," causing IMU-2 to be flagged as failed and the spacecraft to re-enter safe mode. Eventually, IMU-2 came up cleanly.

Investigation showed that the out-of-spec noise on IMU-2 persisted for only a matter of seconds after power-on, so spacecraft-side fault protection settings were adjusted to ignore the initial power-up transient errors. The available data for IMU-1's failed power-on showed the same PLC resets observed previously, along with a gyro condition status of FAILED in the MIMU's status message, which triggered the spacecraft's safe mode. After this, the spacecraft's fault protection was reconfigured so that IMU-1 could no longer be autonomously selected, even in safe mode scenarios.

In April 2022, the gyroless patch was installed on the spacecraft, allowing it to operate with both IMUs powered off. The patch was not designed to operate during propulsive maneuvers or safe mode, the latter being a deliberate tradeoff to meet cost and schedule goals. In February 2023, IMU-2 was commanded to power on and assume control from gyroless mode for a propulsive maneuver, but it immediately triggered a safe mode entry. Telemetry showed IMU-2 had failed a built-in test related to one of the lasers, the SBS test. This marked the first anomalous SBS detection for this unit. Honeywell later clarified that a failed SBS test does not

indicate bad rate data and that the MIMU remains usable in this condition. Following discussions with Honeywell, the project disabled fault protection monitoring of the built-in tests, as Honeywell did not intend it to indicate invalid rate data. IMU-2 was subsequently powered on several times outside the control loop for verification, and it performed normally on each occasion.

The SBS anomalies prompted a campaign to evaluate reintroducing IMU-1 as a last-resort rate source. The conclusion was that IMU-1 might function for a few minutes in a worst-case safe mode scenario, which was considered better than no rate source at all. This fallback contingency, however, was not configured at the time of the anomaly, so the path to IMU-1 was unavailable at the time of the LOS event.

Work on a second gyroless patch capable of operating during safe mode began immediately after the SBS anomalies in 2023 but was still in progress when communications were lost. IMU-2 was estimated to have approximately 20 weeks of laser life remaining, which was considered adequate for maneuver and safe mode activities. MAVEN had been operating successfully in gyroless mode for three years when the mission was lost.

5.5 STEREO-B ANOMALY

About 8 months before the STEREO-B spacecraft was lost in 2014, an anomaly occurred on a similar Honeywell MIMU. The unit was not in the control loop at the time, and data were being recorded and telemetered. The root cause was determined to be “end of cathode life,” meaning the laser could no longer operate. This failure exposed a significant challenge with MIMU fault protection: The unit’s health status messages did not indicate that a laser failure had occurred in the way that STEREO’s software was expecting.

The MIMU provides multiple gyro health and data validity flags. STEREO-B monitored one called the GO/NO-GO bit, which covers all three axes. The expectation during development was that any gyro failure would switch the bit to NO-GO. Instead, the bit indicates GO as long as at least one gyro axis remains functional. There were per-axis status messages that could correctly indicate individual gyro failures, but these messages were not monitored in the interest of keeping the flight software simple.

Since the rate data were still accepted as valid (but not used in the control loop), they were recorded and telemetered. The data showed a sudden transition from a nominal-looking signal to one with a large offset (2.85 deg/s) and significant noise (standard deviation of 1.76 deg/s). With the laser no longer operating, the signal contained no real rate information.

When STEREO-B was lost eight months later, the most likely cause was determined to be a similar failure of its other MIMU, which caused the ACS to spin the spacecraft up, chasing the false rate offset.

5.6 STEREO-B ANOMALY RELATIONSHIP TO MAVEN LOS

MAVEN had the same susceptibility to MIMU laser failure as STEREO-B. MAVEN's post-LOS investigation found that this type of failure would have also caused MAVEN's flight software to accept bad rate data from a failed gyro laser, allowing ACS spin-up to occur. The spin-up could have been prevented if MAVEN had the means to determine that IMU-2 was faulty and been able to switch to the gyroless mode, but these capabilities were not available.

MAVEN had two gyro axes in IMU-2 that were showing laser life decline. It is plausible that, when the spacecraft entered safe mode and IMU-2 was powered, one of its lasers failed in a way similar to what occurred on STEREO-B. This would have produced a similar output: no real rate signal, a significant rate offset, and a status message that MAVEN's software would interpret as valid.

5.7 SIMULATION OF A FAULTY IMU OUTPUT

The LM spacecraft operations team conducted a software simulation of how MAVEN would react to encountering a permanently biased gyro following a spacecraft reboot as hypothesized in the failure scenario above [3].

In the simulated scenario, the injection of a biased gyro signal recreates several phenomena observed in telemetry and via the Doppler signature in the spacecraft downlink following the anomaly. Specifically, a self-induced spacecraft spin is established that the logic in the onboard software is subsequently unable to substantively correct.

Additionally, the resulting timeline of reboot cycles and subsequent rate damping correlates to the radio science observations, with a few discrepancies noted. A significant amount of ΔV is accumulated inertially as a result of these subsequent rate damping events. Additionally, the simulation recreates a signature of slightly decreased rates after each firing of the first secondary thruster suite, followed by a restoration to the original rate after each firing of the second secondary thruster suite, consistent with the behavior observed in the Doppler signature.

6 ROOT CAUSE ASSESSMENT

After eliminating most of the potential failure scenarios from the fishbone assessment, there were only two credible scenarios that remained: (1) An anomalous reboot followed by a failure of IMU-2 that produced an erroneous rate output that caused the ACS to chase the bad data, putting the spacecraft into an unrecoverable tumble, or (2) an external impact to the spacecraft that caused an unrequested reboot and imparted momentum to the vehicle, causing it to tumble in a manner that was unrecoverable by the ACS.

6.1 PROBABILITY OF AN SEU

In most cases of unrequested reboots attributed to SEUs, particularly when the SEU is within a flight computer itself rather than within support electronics such as power supplies, the attribution results not from positive evidence of an SEU (which is usually destroyed when the reboot occurs) but instead after elimination of alternatives in a fishbone analysis. The sole unrequested reboot of a RAD750 computer of design similar to that on MAVEN for which positive evidence of an SEU exists, and which the ARB is aware of, occurred in one of the primary instrument's computers onboard the Fermi Gamma-ray Space Telescope (FGST) in 2020.

In this event, a function executed by one task (A) sent a message to a higher priority task (B), which caused the operating system (OS) to immediately switch execution to B to process the message. Upon completion of that processing, the OS returned control to A. While B was executing, the OS stored A's values of the processor's register set in a data structure adjacent to A's stack. One of A's registers contained a pointer that had been successfully utilized by A prior to the switch to B, but upon return to A, that register contained a corrupted pointer value that caused a memory access violation when subsequently utilized. That corrupted value was effectively captured by processor hardware and included in post-reboot telemetry. The telemetry showed that the corrupted value was the value with which the OS prefills all of a task's stacks when initializing a task. The analysis concluded that, when attempting to restore the register's value from the data structure in which it had been stored when switching to A, an SEU in one of the memory address lines caused the OS to inadvertently access a previously unused portion of the stack adjacent to the data structure rather than the data structure itself.

FGST has continued to operate with no further unrequested reboots attributed to SEUs. It has now accumulated 18 years of operation in low Earth orbit (LEO) on each of its four active RAD750s: one in the spacecraft bus plus three in the primary instrument. This results in a prima facie estimate of the RAD750's unexpected reboot rate from SEUs of 1 event per 72 processor-years, with a 100% error bar on this estimate. Although the radiation environment in MAVEN's Mars orbit is different from FGST's LEO environment, the upset rate for MAVEN is not expected to differ from FGST's rate by multiple orders of magnitude.

Logic design errors associated with unusual "corner cases" within both hardware and software are difficult to discover in flight systems because of the limited number of unit-years of

beta testing performed on these systems prior to launch, as compared to the equivalent testing of commercial data-processing systems prior to offering these systems for sale. Hardware errata are frequently not documented until years after launch of the first unit that encountered a design defect, and even then, the descriptions of possible mitigation schemes are sometimes incomplete, vague, and/or misleading. Often a fishbone analysis fails to include consideration of previously unknown hardware errata, as well as rare timing races in flight software. This occasionally causes the analysis to yield the conclusion of an SEU as root cause without any positive evidence.

The ARB has noted that regardless of the diagnosed root causes of unrequested reboots in other missions, including those operating in the Mars environment, and independent of the correctness of these diagnoses, such reboots do occur at a noticeable rate. While the rate may vary from mission to mission, the mean time between unrequested reboots (regardless of root cause) is typically no more than a few years. Since mankind has not been spacefaring for even a century, there has yet to be a single mission with zero failures in a hundred processor-years.

6.2 External Impact Analysis

To cause the events observed in the MAVEN anomaly, a hypothetical impact by a spacecraft or meteoroid would need to a) knock the spacecraft into the spin that was observed, b) cause an unrequested reboot, c) damage the propulsion system so that it could not damp the spin, and d) leave the spacecraft otherwise in mostly a fully functional state. This would considerably constrain the area on the spacecraft for a strike that could match these criteria.

Meteoroid Impact Analysis

The area on the spacecraft that would need to be struck to cause these events is difficult to assess and would require large numbers of simulations to estimate a credible target area. The size of a meteoroid needed for the impact is similarly difficult to estimate. For purposes of estimating a probability, the ARB chose a meteoroid size of 100 g (about the size of a golf ball) and a required impact zone of about 30 cm by 30 cm.

Using the probability curve in Figure 13 on p. 42 of the NASA document *A Meteoroid Handbook for Aerospace Engineers and Managers* [4], and extrapolating the almost linear curve on the logarithmic plot to 100 g, the probability of an impact would be about 1×10^{-9} per m² per year. For a 30 cm by 30 cm area, this would provide an estimate of about 9×10^{-11}, or roughly one in 10 billion per year. If we were to assume a 10 g meteoroid (the size of a marble), the odds would increase to about one in a billion.

Impact by Another Mars Orbiter

Jordan Isler at JPL examined the estimated orbits of the Mars orbiters that are non-operational, uncontrolled, and unable to be tracked [5]. She considered probability ranges for the Viking 1 and 2 orbiters, Mariner 9, Mars Global Surveyor (MGS), and the Mars Orbiter Mission (MOM).

The Soviet orbiters Mars 3 and 5 were not considered, because we have no trajectory information for them on which to draw from.

For a collision radius of less than 10 m, the cumulative probability of collision from any of the dead orbiters was estimated at about 8×10^{-11} over a 5-year period, or roughly one in 10 billion.

6.3 Assessment of the Most Likely Scenario

Given the disparity in probabilities between the two scenarios identified as credible, the most likely root cause was determined to be an anomalous unrequested reboot followed by the activation of an IMU that was giving an erroneous output for rotation rate. The vehicle responded by spinning up the spacecraft in an attempt to correct the erroneous rate. MAVEN was not able to recover from that state, eventually exhausting available propellant and discharging the battery due to off-pointing from the Sun.

Although this is the most plausible scenario identified, we are not able to definitively state that this was the root cause for the loss of MAVEN.

7 FINDINGS AND RECOMMENDATIONS

7.1 ASSESSMENT OF MAVEN'S ORBIT AND STABILITY

An approximate estimate is that, after 50 years, the MAVEN orbit period will drop by 0.15 hour (from 3.65 to 3.50 hours), and the apoapsis altitude will drop by 370 km (from 4480 to 4110 km). In the following 50 years, it is estimated that these parameters will have a decrease no larger than in the first 50 years, and may be more likely to drop down to just under 3.4 hours in orbit period and 3980 km in apoapsis altitude. Thus, the MAVEN orbit lifetime is expected to be well over 100 years.

Over this period of time, the periapsis altitude should remain stable, oscillating between 210 and 270 km. The orbit orientation and its progression in time should also remain relatively stable.

7.2 ASSESSMENT OF ORBITAL DEBRIS AND POTENTIAL HAZARDS

There is no evidence to indicate that a debris cloud was generated by the anomaly. In the likely case that the vehicle's spin up was caused by faulty IMU data, the spacecraft would be expected to remain completely intact. This is supported by the fact that MAVEN was functioning and transmitting a signal to the Earth for several hours after the initiation of the anomaly.

7.3 ADDRESSING IMU VULNERABILITIES AND END OF LIFE

- **The NASA Engineering and Safety Center (NESC) should review and provide guidance for IMU usage.** The NESC should review this case and make recommendations for IMU health reporting. This might include requiring IMUs to communicate hardware health status and indicate in documentation when rate output should or should not be trusted for control purposes. In addition, it might be recommended to require vendors to include in their specification sheets the expected life under defined operational conditions. These recommendations should be considered for all future NASA missions using the Honeywell MIMU or similar units. NESC has already made some recommendations in their report *Miniature Inertial Measurement Unit (MIMU) Operational Life Investigation* [6].
- **Ensure flight software developers understand MIMU status messages.** Fault protection and software designers must have an accurate understanding of which MIMU status messages should trigger autonomous responses and which should not, supported by improved vendor documentation and communication during development.
- **Improve MIMU interface documentation.** Honeywell should be engaged to improve the MIMU's interface documentation to provide sufficient detail for anomaly planning, including clear guidance on which flags indicate actionable failures versus informational conditions.
- **Improve MIMU thermal operating environment definitions.** Improve MIMU documentation regarding the thermal operating environment, making it clear that

operating units at higher temperatures, even though they are still within current specifications, has a significant negative impact on lifetime.

- **Develop failure simulation capability for hardware-in-the-loop testing.** A mechanism should be established, with vendor coordination, to simulate MIMU failure modes, enabling better fault protection testing during development. The first step would be for Honeywell to provide examples of what outputs to expect from the unit in failure cases, which could then be integrated into simulations.

7.4 GYROLESS MODES OF OPERATION

It is recommended for all Mars orbiters to include a robust gyroless mode of operation as an attitude control option. This should be designed in from the beginning rather than implemented as an add-on after launch. This will enable the preservation of IMU lifetime. Each project should determine the best strategy for the mission as to when the spacecraft should be operating in gyroless mode. Mars orbiters should also implement a robust sun sensor mode as a fallback in which the vehicle could operate in a safe sun-pointing mode using its sun sensors.

A more advanced option would be for the vehicle to have the option of implementing propulsive maneuvers using the gyroless mode rather than having to rely on a usable IMU.

7.5 FAULT PROTECTION RECOMMENDATIONS

It is recommended to have fault protection that has features to recognize when an IMU output indicates a high rate of rotation when that would not be expected. The software could compare that rate with inputs from the star trackers and sun sensors to make a decision on trusting the IMU or switching to a gyroless star tracker or sun sensor mode of attitude determination.

Mars orbiters should also have the option of configuring safe mode to be initiated in gyroless mode rather than on an IMU.

7.6 SPACE SITUATIONAL AWARENESS AT MARS

As more spacecraft orbit Mars, there will inevitably be an increase in the number of derelict (non-communicative) vehicles, and eventually their debris. At the moment, there is no effective means of tracking these objects at Mars.

Just as Mars orbiters have been required to carry relay radios, some future Mars orbiters should be required to carry cameras that are suitable for detecting and tracking other objects in Mars orbit. After the initial orbit of an object is determined, only occasional observations would be needed for updating the ephemerides. While searching for long-lost objects is much harder, there are still not that many objects to find, such that a modest observing cadence and duration should suffice to find everything present. Afterward, the orbital update phase could be rather minimal.

A notional camera system concept could use a narrow-angle framing camera on a two-axis gimbal to make low-phase observations of near-Mars space. Such a system could also be useful for scientific observations. It might be useful to include onboard object detection capability to reduce the downlink data volume.

APPENDICES

A Convening Memo

B Integrated Timeline of Anomaly Events

C Acknowledgment

D Acronyms

E References

APPENDIX A Convening Memo

National Aeronautics and
Space Administration
Mary W. Jackson Building NASA Headquarters
Washington, DC 20546-0001



Reply to Attn of: Science Mission Directorate/Planetary Science Division

TO: Director, Planetary Science Division

FROM: Associate Administrator for Science Mission Directorate

SUBJECT: Anomaly Review Board formulation for the MAVEN mission

This memo is in response to the Planetary Science Division (PSD) request to form an anomaly review board (ARB) for the Mars Atmosphere and Volatile Evolution (MAVEN) mission. Given the last successful communication with MAVEN was on December 4, 2025 and attempts to regain contact have been unsuccessful, please formulate a MAVEN ARB.

Please ensure the charter to the ARB includes:

1. An evaluation of the MAVEN team's recovery efforts including identification of any feasible alternative approaches. This evaluation should include an assessment of the likelihood of recovery.
2. An assessment of the potential outcomes and most likely state of the MAVEN spacecraft. This assessment should include identification of any risks or residual risks associated with the anomaly.
3. An evaluation of the MAVEN team's root cause investigation including identification of alternative causes.
4. Identification of lessons learned that are applicable to other NASA assets, including current or future missions.

I concur with the PSD recommendation for expertise and personnel, namely:

Chair: Hoppy Price (JPL), Mars Exploration Program Office Chief Engineer
Senior Advisor to Chair: Carmel Conaty (HQ), SMD Chief Engineer
Project Management, Science: Joel Krajewski (Univ California, Berkeley)
Flight Systems: Chris Waters (Lockheed Martin)
Flight Operations: Devin Poland (GSFC)
Guidance, Navigation & Control: Liam Pisano (Infinite Horizon Company)
Safety & Mission Assurance: Jesse Bullock (GSFC)
Avionics: Eric Siskind (NYCB Realtime Computing)
Navigation: Tim McElrath (JPL)
Systems Engineering, Mars Missions: Charles Whetsel (JPL)

I request that PSD keep SMD leadership informed when key milestones are reached by the ARB and look forward to the initial briefing to SMD no later than three months from the start of the ARB's work. The initial briefing should include applicable findings regarding probable state of the spacecraft and the likelihood of recovery. A final report should be delivered no later than six months from the start of the ARB's work.

Nicola Fox Digitally signed by Nicola Fox
Date: 2026.02.16 12:14:05 -05'00'

Nicola J. Fox, PhD

CC:
HQ/SMD DAA (M. Clampin)
HQ/SMD DAAP (W. Peters)
HQ/SMD Information Security (J. Esper)
HQ/SMD PSD Deputy (C. Webb)
HQ/SMD MEP Director (T. Morgan)
HQ/SMD MAVEN PE (M. Fujieh)
HQ/SMD MAVEN PS (R. Fogel)
HQ/SMD OComms (K. Fox)
HQ/SMD PSD OComms (A. Johnson)
HQ/SMD OIIR (M. Dalby)
GSFC/100 (C. Simmons)
GSFC/300 (D. Healey)
GSFC/400 (C. Richards)
GSFC/444 (B. Grofic)
GSFC/444 (M. Moreau)
GSFC/500 (S. Harris)
GSFC/531 (J. Gregory)
GSFC/531 (N. Castro)
JPL/Mars Exploration Program Office (J. Parrish)
JPL/Mars Exploration Program Office (H. Price)
LASP/Principal Investigator (S. Curry)

APPENDIX B Integrated Timeline of Anomaly Events

ERT	Observed/Inferred Events	Speculated Events	Source	Notes
1:46	Last telemetry, pre-occultation		DSN	Spacecraft in nominal expected condition
1:57	Last signal, pre-occultation		DSN	
1:58	Enter occultation		Orbital prediction	
2:00	Enter eclipse		Orbital prediction	
2:06		Initial fault	guess	Based on the allowable time window
2:07	**Reboot 0 - unrequested, cold**		analysis of telemetry	
2:08	Safe mode entry - reboot recovery		analysis of telemetry	
2:11		**ΔV event (ACS only)**	based on ACPM cycle	ACPM = Attitude Control Performance Monitor
2:12	Safe mode entry - ACPM fault		analysis of telemetry	S/C is probably tumbling at this point
2:15		**ΔV event (ACS only)**	based on ACPM cycle	
2:16	Safe mode entry - ACPM fault		analysis of telemetry	
2:19		**ΔV event (ACS+TCM)**	based on ACPM cycle	
2:20	Safe mode entry - ACPM fault		analysis of telemetry	
2:23		**ΔV event (ACS+TCM)**	based on ACPM cycle	
2:24	Safe mode entry / reboot request - ACPM		analysis of telemetry	
2:27	**Reboot 1 - requested, warm**		analysis of telemetry	
2:28	Safe mode entry - reboot recovery		analysis of telemetry	
2:29	Exit eclipse and occultation		Orbital prediction	
2:31		**ΔV event (ACS only)**	based on ACPM cycle	
2:32	Safe mode entry - ACPM fault; **roll rate ~2.7 rpm**		analysis of telemetry	Safe mode timelines line up with ACPM rate error fault
2:33	**Roll rate ~2.7 rpm**		LM analysis based on signal strength	
2:35		**ΔV event (ACS only)**	based on ACPM cycle	
2:36	Safe mode entry - ACPM fault		analysis of telemetry	
2:37	**Roll rate ~2.6 rpm**		LM analysis based on signal strength	
2:39	**ΔV event (ACS+TCM)**		Doppler analysis	LGA offpoint correlation averages about 45 deg
2:40	Safe mode entry - ACPM fault		analysis of telemetry	
2:41	**Roll rate ~2.3 rpm**		LM analysis based on signal strength	
2:44	**ΔV event (ACS+TCM); roll rate ~2.7 rpm**		Doppler analysis; signal strength	LGA offpoint correlation averages about 45 deg
2:45		Safe mode entry / reboot request - ACPM	based on ACPM cycle	
2:48		**Reboot**	based on ACPM cycle	
2:52		**ΔV event (ACS only)**	based on ACPM cycle	
2:53	**Roll rate ~2.7 rpm**	Safe mode entry - ACPM fault	based on ACPM cycle; signal strength	
2:56		**ΔV event (ACS only)**	based on ACPM cycle	
2:57	**Roll rate ~2.6 rpm**	Safe mode entry - ACPM fault	based on ACPM cycle; signal strength	
3:00	**ΔV event (ACS+TCM)**		Doppler analysis	LGA offpoint correlation averages about 40 deg
3:01	**Roll rate ~2.3 rpm**	Safe mode entry - ACPM fault	based on ACPM cycle; signal strength	
3:04	**ΔV event (ACS+TCM)**		Doppler analysis	LGA offpoint correlation averages about 40 deg
3:05	**Roll rate ~2.7 rpm**	Safe mode entry / reboot request - ACPM	based on ACPM cycle; signal strength	

ERT	Observed/Inferred Events	Speculated Events	Source	Notes
3:09		Reboot	based on ACPM cycle	
3:13		ΔV event (ACS only)	based on ACPM cycle	
3:14		Safe mode entry - ACPM fault	based on ACPM cycle	
3:15	Roll rate ~2.7 rpm		LM analysis based on signal strength	
3:16		ΔV event (ACS only)	based on ACPM cycle	
3:18	Roll rate ~2.6 rpm	Safe mode entry - ACPM fault	based on ACPM cycle; signal strength	
3:21	ΔV event (ACS+TCM)		Doppler analysis	LGA offpoint correlation averages about 45 deg
3:22	Roll rate ~2.3 rpm	Safe mode entry - ACPM fault	based on ACPM cycle; signal strength	
3:25	ΔV event (ACS+TCM); roll rate ~2.7 rpm		Doppler analysis; signal strength	LGA offpoint correlation averages about 45 deg
3:26		Safe mode entry / reboot request - ACPM	based on ACPM cycle	
3:29		Reboot	based on ACPM cycle	
3:33		ΔV event (ACS only)	based on ACPM cycle	
3:34		Safe mode entry - ACPM fault	based on ACPM cycle	
3:35	Roll rate ~2.7 rpm		LM analysis based on signal strength	
3:37		ΔV event (ACS only)	based on ACPM cycle	
3:38		Safe mode entry - ACPM fault	based on ACPM cycle	
3:39	Roll rate ~2.6 rpm		LM analysis based on signal strength	
3:41	ΔV event (ACS+TCM)		Doppler analysis	LGA offpoint correlation averages about 55 deg
3:42		Safe mode entry - ACPM fault	based on ACPM cycle	
3:43	Brief carrier lock		DSN	
3:43	Roll rate ~2.4 rpm		LM analysis based on signal strength	
3:45	ΔV event (ACS+TCM)		Doppler analysis	LGA offpoint correlation averages about 55 deg
3:46		Safe mode entry / reboot request - ACPM	based on ACPM cycle	After this time, roll rate not estimated due to noisy data
3:50		Reboot	based on ACPM cycle	
3:54		ΔV event (ACS only)	based on ACPM cycle	
3:55		Safe mode entry - ACPM fault	based on ACPM cycle	
3:58		ΔV event (ACS only)	based on ACPM cycle	
3:59		Safe mode entry - ACPM fault	based on ACPM cycle	
4:02		ΔV event (ACS+TCM)	based on ACPM cycle	
4:03		Safe mode entry - ACPM fault	based on ACPM cycle	
4:06	ΔV event (ACS+TCM)		based on ACPM cycle	LGA offpoint correlation averages about 55 deg
4:07		Safe mode entry / reboot request - ACPM	based on ACPM cycle	
4:11		Reboot	based on ACPM cycle	
4:14		ΔV event (ACS only)	based on ACPM cycle	
4:15		Safe mode entry - ACPM fault	based on ACPM cycle	
4:18		ΔV event (ACS only)	based on ACPM cycle	
4:19		Safe mode entry - ACPM fault	based on ACPM cycle	
4:22		ΔV event (ACS+TCM)	based on ACPM cycle	
4:23		Safe mode entry - ACPM fault	based on ACPM cycle	
4:26		ΔV event (ACS+TCM)	based on ACPM cycle	
4:27		Safe mode entry / reboot request - ACPM	based on ACPM cycle	

ERT	Observed/Inferred Events	Speculated Events	Source	Notes
4:31		**Reboot**	based on ACPM cycle	
4:35		**ΔV event (ACS only)**	based on ACPM cycle	
4:36		Safe mode entry - ACPM fault	based on ACPM cycle	
4:39	**ΔV event (ACS only)**		based on ACPM cycle	LGA offpoint correlation averages about 65 deg
4:40		Safe mode entry - ACPM fault	based on ACPM cycle	
4:41	Last signal positively received from S/C		OLR data	
4:43		**ΔV event (ACS+TCM)**	based on ACPM cycle	
4:44		Safe mode entry - ACPM fault	based on ACPM cycle	
4:47		**ΔV event (ACS+TCM)**	based on ACPM cycle	
4:48		Safe mode entry / reboot request - ACPM	based on ACPM cycle	
4:51	Weak signal received		OLR data	
4:52		**Reboot**	based on ACPM cycle	
4:55		**ΔV event (ACS only)**	based on ACPM cycle	
4:56		Safe mode entry - ACPM fault	based on ACPM cycle	
4:59		**ΔV event (ACS only)**	based on ACPM cycle	
5:00		Safe mode entry - ACPM fault	based on ACPM cycle	
5:03		**ΔV event (ACS+TCM)**	based on ACPM cycle	
5:04		Safe mode entry - ACPM fault	based on ACPM cycle	
5:08		**ΔV event (ACS+TCM)**	based on ACPM cycle	
5:09		Safe mode entry / reboot request - ACPM	based on ACPM cycle	
5:11		Reboot not accepted due to fault protection dead end	Based on fault protection design	No more spacecraft reboots expected after this point
5:12		**ΔV event (ACS+TCM)**	based on ACPM cycle	
5:13		Control error fault	based on ACPM cycle	
5:16		**ΔV event (ACS+TCM)**	based on ACPM cycle	
5:17		Control error fault	based on ACPM cycle	
5:20		**ΔV event (ACS+TCM)**	based on ACPM cycle	
5:21		Control error fault	based on ACPM cycle	
5:24		**ΔV event (ACS+TCM)**	based on ACPM cycle	
5:25		Control error fault	based on ACPM cycle	
5:28		**ΔV event (ACS+TCM)**	based on ACPM cycle	
5:29		Control error fault	based on ACPM cycle	
5:32		**ΔV event (ACS+TCM)**	based on ACPM cycle	
5:33		Control error fault	based on ACPM cycle	
5:33	Signal potentially received from S/C		OLR data	
5:36		**ΔV event (ACS+TCM)**	based on ACPM cycle	
5:37		Control error fault	based on ACPM cycle	

ERT	Observed/Inferred Events	Speculated Events	Source	Notes
5:37	Enter occultation		Orbital prediction	
5:38	Enter eclipse		Orbital prediction	
5:40		**ΔV event (ACS+TCM)**	based on ACPM cycle	
5:41		Control error fault	based on ACPM cycle	
5:44		**ΔV event (ACS+TCM)**	based on ACPM cycle	
5:45		Control error fault	based on ACPM cycle	
5:48		**ΔV event (ACS+TCM)**	based on ACPM cycle	
5:49		Control error fault	based on ACPM cycle	
5:52		**ΔV event (ACS+TCM)**	based on ACPM cycle	
5:53		Safe mode entry dead end	based on ACPM cycle	
5:55		**Stuck in rate damping attempts (ACS+TCM)**	based on ACPM cycle	
5:58		**Re-occuring thruster fault cycle repeating every 3 minutes**	based on ACPM cycle	
5:07	Exit eclipse		Orbital prediction	
6:08	Exit occultation		Orbital prediction	
6:10	Beginning of last signal potentially received		OLR data	
6:20	End of last signal potentially received		OLR data	LGA offpoint correlation averages about 60 deg
8:30		Estimated earliest time for when battery would be dead	Power Subsystem estimate	Estimated off-point of solar array inferred from LGA offpoint
11:00		Estimated mean time for when battery would be dead	Power Subsystem estimate	Estimated off-point of solar array inferred from LGA offpoint
16:00		Estimated latest time for when battery would be dead	Power Subsystem estimate	Estimated off-point of solar array inferred from LGA offpoint
23:09	Command sent to exert downlink state		DSN transmit	

APPENDIX C Acknowledgment

The ARB would like to acknowledge the following groups and individuals for their help during its investigation.

- The MAVEN project has been extremely helpful in providing support and analyses to the ARB.
- Lockheed Martin has provided important information to the ARB for determining spacecraft state, timelines, and fault protection design and investigating failure scenarios.
- The Deep Space Network has provided outstanding support in searching for signals from MAVEN and transmitting commands in attempts to recover the vehicle.
- The Green Bank Observatory provided attempts to receive signals from MAVEN, and the results of those searches, although negative, are important to the ARB's findings.
- The MAVEN radio science team and the navigation team provided essential data and analyses that have been instrumental to the investigation.
- The European Space Agency has generously used their Trace Gas Orbiter (TGO) spacecraft in attempts to image MAVEN.

APPENDIX D Acronyms

This section provides acronyms used in this report. The acronyms listed below span the body of this report and also cover items relevant to the appendices, as well as acronyms used in the illustrations of this report.

ACRONYMS

ACPM	attitude control performance monitor
ACS	attitude control system
APP	articulated payload platform
ARB	Anomaly Review Board
DSN	Deep Space Network
ERT	Earth-received time
FGST	Fermi Gamma-ray Space Telescope
GSFC	Goddard Space Flight Center
HGA	high-gain antenna
IMU	inertial measurement unit
LEO	low Earth orbit
LGA	low-gain antenna
LIM	laser intensity monitor
LM	Lockheed Martin
LOS	loss of signal
MAVEN	Mars Atmosphere and Volatile Evolution
MGS	Mars Global Surveyor
MIMU	miniature inertial measurement unit
MOI	Mars orbit insertion
MOM	Mars Orbiter Mission
NESC	NASA Engineering and Safety Center
OLR	open-loop recording
OS	operating system
PLC	path length control
RCS	reaction control system
RLG	ring-laser gyroscope
RPM	revolutions per minute
S/C	spacecraft

SBS	single-beam signal
SEU	single-event upset
TCM	trajectory correction maneuver
TGO	Trace Gas Orbiter
UTC	Coordinated Universal Time

APPENDIX E References

[1] Demcak, Stuart. 15 May 2026. “Navigation Analyses for the MAVEN Loss of Signal after the 12/6/2025 Occultation.” JPL internal presentation.

[2] Lockheed Martin. 16 April 2026. “MAVEN Spacecraft Anomaly: LM Investigation.” Internal presentation.

[3] Kennedy, Tom. 2026. “Bad IMU Output: GN&C Analysis.” Lockheed Martin internal presentation.

[4] Cooke, William J., and Althea V. Moorhead. 2019. *A Meteoroid Handbook for Aerospace Engineers and Managers*. NASA/TM-2019-220142. Huntsville, AL: NASA Meteoroid Environments Office.

[5] Isler, Jordan. 2 February 2026. “MAVEN Collision Analysis.” JPL internal presentation.

[6] NASA. 30 June 2022. *Miniature Inertial Measurement Unit (MIMU) Operational Life Investigation*. NESC technical report.